The SWP Echelle Ripple Correction Revisited

C.A. Grady and M.P. Garhart

July 1, 1988

I. INTRODUCTION

One of the distinguishing characteristics of echelle spectra is the large variation in sensitivity as a function of wavelength within each spectral order. Compensation for this variation is an essential part of the reduction of IUE high dispersion spectra to the form of relatively or absolutely calibrated fluxes as a function of wavelength. As currently implemented in IUESIPS, the echelle blaze, or "ripple" correction, is applied immediately following spectral extraction, and compensates both for the sensitivity variation of the spectrograph, and any residual flat field effects in the camera (Turnrose and Thompson 1984). Ake (1982) in analyzing the LWR and SWP ripple corrections noted that camera sensitivity degradation could signficantly distort the measured shape of the echelle blaze function, and that the ripple correction should be re-evaluated at intervals. At the time of his analysis, no significant changes in the SWP sensitivity, and hence in the ripple function, had been noted. An additional six years have passed since the time of Ake's analysis, and the SWP camera is now known to show a significant loss of sensitivity compared to the launch epoch.

II. FUNCTIONAL FORM OF THE RIPPLE FUNCTION

Ake (1982) found that the wavelength dependence of the variation in sensitivity within an SWP high dispersion order could be fit by

$$R(\lambda) = sinc^2(\frac{\pi m \alpha |\lambda - K/m|}{\lambda}) \tag{1}$$

where m is the echelle spectral order number, K is a parameterized form of the echelle grating constant, α is an adjustable parameter, and sinc(x)=sin(x)/x. Ake found the best fit to the observed sensitivity variation within each spectral order by allowing

$$K = a_0 + a_1 m + a_2 m^2 \tag{2}$$

and α=0.856±0.03. Too few high dispersion spectra were available at the time of his analysis to determine whether the ripple function depended on other factors.

III. CHOICE OF DATA

We have restricted our analysis to IUE calibration spectra processed between 1982 March and 1988 January. This time range was chosen to exclude data processed under early versions of the IUESIPS, since those spectra are subject to potentially large extraction errors. Tables 1 and 2 list the 67 spectra included in the study, as well as information on camera temperatures, and exposure level at the time of observation. These spectra were supplemented by η UMa linearity monitoring observations which were not included in the final ripple correction.

IV. ANALYSIS TECHNIQUE

Ake's (1982) initial analysis of the ripple function of the SWP echelle involved least squares fitting of the observed sensitivity variations within an order to the function given in equation 1, with K a free parameter determined by fitting. All spectral data within the order which were not flagged as poor quality data were used. This approach, while comparatively simple to implement, and having the advantage that each order can be fit independently, is affected by the presence of spectral lines, particularly in the regions of maximum camera sensitivity. Inspection of the mean K values in Ake (1982) shows that the largest scatter from values in adjacent orders occurs in orders containing strong resonance lines such as C IV, Si IV, and Lyman α. Much of the curvature in the quadratic fit to K(m) derived by Ake (1982) is due to these large order-to-order deviations in the mean K values derived using the least squares fitting technique.

An alternate approach, which is less sensitive to nature of the calibration source, was developed by Barker (1984). In this technique the K values are adjusted to minimize the differences in the ripple-corrected net fluxes in the region of wavelength overlap between successive orders. This technique is not sensitive to the presence of spectral features, since the same features should occur at the same wavelengths in successive orders. The Barker technique is very sensitive to the presence of noise in the spectra, and generally will not work well for poorly exposed spectra, or spectra containing only isolated emission lines. We have used the Barker technique to derive K values for all orders with appreciable wavelength overlap, this has meant restricting our analysis to SWP orders 72-124, and ignoring the orders contaminated by interstellar Lyman α.

V. REPRODUCIBILITY OF K VALUES

Previous studies of the Barker technique (Barker 1984) demonstrated the utilitity of

this approach for ripple correcting individual high dispersion spectra of early-type stars. No evaluation of the reproducibility of the K values derived by this technique had been made, nor an evaluation of the sensitivity of the derived K values to exposure conditions. Since we intend to use K values derived via the Barker technique to be applied to spectra other than the spectra for which the data were derived, this kind of evaluation is essential.

a) Reproducibility for Identical Observations

We have compared 5 optimally exposed spectra of η UMa obtained and processed in 1987-1988 with 5 spectra obtained and processed in 1982 and 1983. All spectra were chosen to have similar exposure times, exposure characteristics, and were obtained with THDA=10.5. Figure 1 a shows mean K values (solid line) and K values from individual spectra (dots) for the 1982-1983 spectra. With the exception of the region in orders 113-114, which is affected by Lyman α, and the highest orders, the individual spectra K values differ from the mean by at most 15. Figure 1b shows similar data from 1987-1988. Figure 1c is a comparison of the 1982-1983 and 1987-1988 data. The mean K values from each year do not differ significantly. We do not find evidence for any change in the ripple parameter for identical images obtained over the past six years. This analysis should be extended to earlier spectra once such data have been reprocessed.

b) Reproducibility of K values for different exposure levels

We have explored the applicability of the K values derived from optimally exposed η UMa spectra to spectra which have been systematically underexposed or overexposed. Figure 2 shows the K values as a function of order number for 4 spectra obtained sequentially on 1988 Jan 1 to 2. The exposure levels range from C=105 for SWP 32651 to C=1.5X for SWP 32654. The optimally exposed ($*$ and $\diamond$) and overexposed (Δ) spectra have K values which are in good agreement. The underexposed spectrum (+) shows large deviations from the K values derived for the other spectra, and from the mean K values shown in Figure 1. This effect is particularly pronounced at longer wavelengths, where the B3 spectrum is less heavily exposed, and at the shortest wavelengths where camera sensitivity is low. The lack of sensitivity to this modest level of overexposure is a result of the Barker technique relying on the less heavily exposed, and hence unsaturated, portions of each spectrum. The Barker technique is clearly sensitive, however, to signficant underexposures, particularly in the less well exposed parts of the spectrum.

Next we have considered how applicable ripple K values derived from IUE spectra of a single object are for correcting spectra of other objects. Figure 3 shows K values as a function of order number for 4 of the PHCAL targets, HD 87901 (B7) (Δs), HD 3360 (B2) ($\diamond$s), τ Sco (B0) and HD 34816 (B0)($*$), and BD+28 4211 (sdO) (+). All of the spectra considered here are contemporary with the 1987-1988 η UMa observations, and were obtained with THDA=10.5. The spectra of HD 3360, and HD 38416 were exposed to C=182 and 165 respectively. The spectrum of HD 87901 was exposed to C=211 near 1800 Å, and is compared with SWP 32651. The largest differences from the η UMa mean K values are seen for BD +28 4211 at the longer wavelengths, where this spectrum was significantly underexposed, and at the very shortest wavelengths where the low sensitivity of the IUE results in poor reproducibility of the K values derived using the Barker technique. This analysis suggests that mean K values derived by averaging over the PHCAL targets will be applicable to a comparatively wide range of spectral types and flux distributions.

c) Reproducibility for Spectra Obtained with Different THDA

Not all IUE spectra are obtained with the same camera temperature. Sensitivity monitoring has shown that the mean THDA for spectra obtained in the past few years is considerably higher than the mean THDA for the data included in Ake's (1982) analysis. Figure 4 shows the effect on the K values of varying the THDAs. K values for two spectra with 6.5$\leq$THDA$\leq$7.5 are shown as + signs. The mean η UMa K values (THDA=10.5) are shown as the solid line. This temperature is typical of the majority of IUE high dispersion spectra obtained since 1982. A spectrum with THDA=11.2 is shown as $\diamond$s. These results indicate that while differences in THDA of $\pm$1-2 degrees do not significantly affect the mean K values, larger ranges in THDA result in systematic displacements in all of the K values for a particular image. As a result, we propose deriving a ripple correction with mean THDA=10.5, typical of recent images, and a ripple correction with a lower THDA. Should the average THDA values continue to increase, as is anticipated for the 1 gyro control system, the SWP ripple correction will need to be revised.

VI. MEAN RIPPLE K PARAMETERS

Figure 5a shows the mean of 51 optimally exposed spectra of eight calibration stars chosen to have 9.5$\leq$THDA$\leq$11.5. Each calibration star included is represented by at least 3 spectra, although the most frequently observed high dispersion calibration standard η UMa

is represented by 12 spectra in this average. The mean K values are indicated by diamonds. The error bars indicate the 1 σ scatter in the K values. The solid line is a quadratic least squares fit to the mean K values. All orders included in the fit lie within 1σ of the polynomial fit. Figure 5b is a comparison of the revised THDA=10.5 fit with the polynomial fit derived by Ake (1982). We find

$$K(m) = 137730.0 - 3.0644019m + 0.0335206184m^2. \quad (3)$$

Due to the gradual increase in THDA for SWP spectra, many fewer low THDA calibration spectra have been obtained and processed since 1982 March. Figure 6a shows the mean of 16 optimally exposed spectra of 5 calibration stars chosen to have 5.5≤THDA≤7.5. Figure 6b compares the low THDA fit with the THDA=10.5 fit, and with the Ake (1982) fit. For 5.5≤THDA≤7.5 we find

$$K(m) = 137457.97 + 2.3445991m + 0.00557386644m^2. \quad (4)$$

VII. PHOTOMETRIC CONSEQUENCES

Changing the ripple constants can have dramatic photometric consequences for SWP high dispersion spectra. We have compared the performance of the ripple correction at 1206Å, 1570Å, and 1890Åfor 5 SWP spectra of B stars. Two of the stars, HD 36486 (O9II) and γ Cas (B0.5) have comparatively early spectral types, and hence are optimally exposed at 1300 Å . The γ Cas spectrum was obtained with THDA=6.6, and provides an opportunity to test the applicability of the THDA=10.5 correction to cooler camera temperatures. Two of the stars are mid- to late-type B stars and are optimally exposed at 1800Å. The remaining spectrum is of a B9 star, and is 2.5 overexposed at the longest wavelengths. This spectrum was also obtained with THDA=13.8, and thus is atypically hot for SWP camera temperatures obtained to date. Figure 7 shows the region around 1206, 1570, and 1890 Å for HD 36486. We find that the revised THDA=10.5 ripple correction outperforms the Ake (1982) function in all of these test spectra, resulting in flatter spectra with reduced flux discontinuites at the order boundaries in all three test bandpasses. At 1206 Å the THDA=10.5 correction reduces the amplitude of a spurious absorption/emission feature at 1204 A by 20%. At 1570 Å the new correction increases fluxes at the short wavelength end of each order by 4%, and decreases fluxes at the long wavelength end by 4%. At 1890 Å the new correction decreases fluxes by 2% at the short wavelength end of each order, and increases fluxes by 7% at the

long wavelength end, resulting in smaller flux discontinuities at the order overlaps and across the gaps in the spectrum.

VIII. DISCUSSION

The parameterization for K as a function of order number shown in equation (3) results in an improved ripple correction for stars ranging from O to early A spectral types, and THDAs typical of the majority of IUE observations. This ripple correction is uniformly valid for spectra obtained since 1982 March; the suitability of this correction for earlier data is not known, but will be the subject of ongoing investigations. This ripple correction is intimately dependent upon the details of the application of the ITF to the spectral image, as shown by the dependence of K values upon exposure level. It is equally sensitive to the spectral extraction technique as shown by the dependence upon THDA. Bianchi and Bohlin (1984) evaluated straylight effects for SWP spectra of sources which had been observed by *Copernicus*. They found a roughly linear relation between the amplitude of the straylight and order number for orders shortward of 1400 Å (order 100). This is similar to the dependence of the ripple parameter on order number which we have found for spectra processed since 1982 March. This kind of strong dependence of the ripple K parameter on order number is not expected for an echelle spectrograph, and is likely to reflect the presence of straylight in the net spectrum. As a consequence, any significant revisions to the way IUE high dispersion spectra are processed, such as inclusion of an inter-order light correction in IUESIPS, modification to the spectral extraction, or use of different photometric corrections for IUE spectra are likely to invalidate this ripple correction.

A by-product of this study has been an analysis of the ripple correction technique. Our results indicate that the Barker technique is suitable for optimally exposed spectra of continuous sources. Weak spectra, or spectra dominated by noise produce abnormally high K parameters, which simply reflect the dilution of the spectrum by noise, and may not be physical. Such spectra may be better calibrated using mean ripple parameters, such as we have derived above.

REFERENCES

Ake, T.B. 1982, *NASA IUE Newsletter*, **19**, 37.

Barker, P.K. 1984, *A. J.*, **89**, 899.

Bianchi, L. and Bohlin, R.C. 1984, *Astr. Ap.*, **134**, 31.

Turnrose, B.E. and Thompson, R.W. 1984, *International Ultraviolet Explorer Image Processing Information Manual, Version 2.0 (New Software)*, CSC/TM-84/6058.

Table 1 - High THDA Calibration Spectra

Star Name	SWP	Spec. Type	THDA	C	B
ζ Cas	27198	B2IV	11.2	180	35
	27379		10.5	190	35
	27543		9.8	190	35
	28627		10.2	190	32
	31525		9.8	186	35
	32365		10.5	182	35
HD 34816	26570	B0IV	9.8	170	35
	26726		10.8	205	35
	29771		9.8	160	32
	30177		9.5	170	35
	32364		10.8	174	34
HD 60753	25399	B3IV	10.2	190	30
	27200		10.5	180	36
	27215		9.8	211	40
	28771		9.8	185	37
	30431		9.8	180	31
BD +75 325	25531	sdO	10.5	150	35
	26963		9.8	201	40
	27374		9.8	175	38
	27416		11.2	214	35
	30032		9.8	198	40
	30084		9.5	180	40
HD 93521	24759	O9Vp	10.8	187	35
	26060		11.2	172	30
	30086		9.8	165	30
τ Sco	25320	B0V	11.5	210	37
	25829		9.5	215	35
	28628		9.5	204	35
	30608		10.8	175	35
BD+28 4211	26964	sdO	10.2	234	40
	29783		9.8	180	35
	29869		11.8	238	30
	29925		10.8	238	42
	31094		10.2	218	51
	32534		10.8	199	34
η UMa	16714	B3IV	10.5	180	32
	18423		10.5	180	33
	18444		10.5	180	30
	18882		10.8	174	30
	18926		11.8	170	35
	19033		10.5	180	32
	19399		10.8	180	32
	19596		11.2	...	...
	19916		10.8	180	31
	21713		10.5	...	...
	24730		11.5	170	35
	30905		10.8	170	32
	31104		10.5	174	32
	31288		10.5	170	32
	31289		10.5	195	35
	32651		10.5	205	38

Table 2 - Low THDA Calibration Spectra

Star Name	SWP	Spec. Type	THDA	C	B
HD 34816	26953	B0IV	6.5	180	37
	32709		6.5	165	32
HD 60753	26636	B3IV	5.1	187	38
	26637		5.8	186	36
τ Sco	26632	B0V	7.5	180	36
	29317		7.5	220	33
	30474		7.8	190	35
BD +28 4211	28491	sdO	6.8	165	40
	29114		5.1	230	40
η UMa	16574	B3V	6.5	...	...
	20374		7.2	180	32
	22469		7.2	175	32
	27046		7.5	170	32
	30434		7.8	175	35
	31065		7.8	170	35
	32712		5.8	170	34

FIGURE CAPTIONS

Figure 1: Lack of time dependence in K values:

a) Mean K values for 1982-1983 spectra are shown by a solid line. The individual spectrum K values are shown as points.

b) Mean K values for 1987-1988 spectra displayed as in Figure 1a.

c) Comparison of 1982-1983 and 1987-1988 K values. The individual spectra are shown as points. The mean K values for each year are shown as + signs. The mean 1982-1983 and 1987-1988 K values are shown as a solid line. The individual year means lie within one σ of the overall mean, indicating no time dependence in the K values.

Figure 2: K values derived using the Barker (1984) technique depend upon exposure level. The optimally exposed ($*$ and $\diamond$) and overexposed (C=1.5X Δ) spectra have K values which are in good agreement. The underexposed spectrum (C=105, +) shows large deviations from the K values derived for the other spectra, and from the mean K values shown in Figure 1.

Figure 3: Dependence of K value on spectral type: HD 87901 (B7) (Δs), HD 3360 (B2) ($\diamond$s), τ Sco (B0) and HD 34816 (B0)($*$), and BD+28 4211 (sdO) (+).

Figure 4: Dependence upon THDA: K values from spectra with 6.5$\leq$THDA$\leq$7.5 are shown as + signs. The mean η UMa K values (THDA=10.5) are shown as the solid line. A spectrum with THDA=11.2 is shown as $\diamond$s.

Figure 5: High THDA ripple correction:

a) Mean K values derived using the Barker (1984) technique for 51 optimally exposed spectra of 8 IUE calibration stars with 9.5$\leq$THDA$\leq$11.5. The mean K values are shown as $\diamond$s. Plus or minus 1σ uncertainties are shown in the error bars. The quadratic least squares fit to the mean K values is shown as the solid line.

b) Comparsion of the high THDA correction (broad solid line) with the quadratic fit derived by Ake (1982).

Figure 6: Low THDA ripple correction:

a) Mean K values, error bars and quadratic fit are shown using the same convention as in Figure 5a for spectra with mean THDA=6.2.

b) Comparison of the high THDA mean K values Δs and quadratic fit, with the low THDA mean K values $\diamond$s and quadratic fit, and with Ake (1982) quadratic fit.

Figure 7: Comparison of spectra processed with the Ake (192) and high THDA ripple corrections. The heavy line indicates data processed with the THDA=10.5 correction, while the light line is the Ake (1982) correction.

a) The 1026 Å region in HD 36486 (O9 II). The largest change is seen at the order boundary at 1204 Å.

b) The 1545-1570 Å region in HD 36486. Differences of a few percent are present near the order boundary at 1555 Å.

c) The 1890-1910 Å region in HD 36486. The new correction produces a spectrum which is flatter across the order boundary at 1902 Å.

d) The 1206 Å region in a spectrum of γ Cas obtained with THDA=6.6. The THDA=10.5 correction removes the spurious absorption feature at 1204 Å.

e) The 1555 Å region in γ Cas shows improvements similar to those seen in HD 36486.

f) The 1900 Å region in γ Cas is flatter with the new ripple correction.

g) The 1555 Å region in an overexposed spectrum of σ Her.

h) The 1900 Å region in the overexposed spectrum of σ Her. Saturated portions of the spectrum are shown with os.

Figure 1a-c

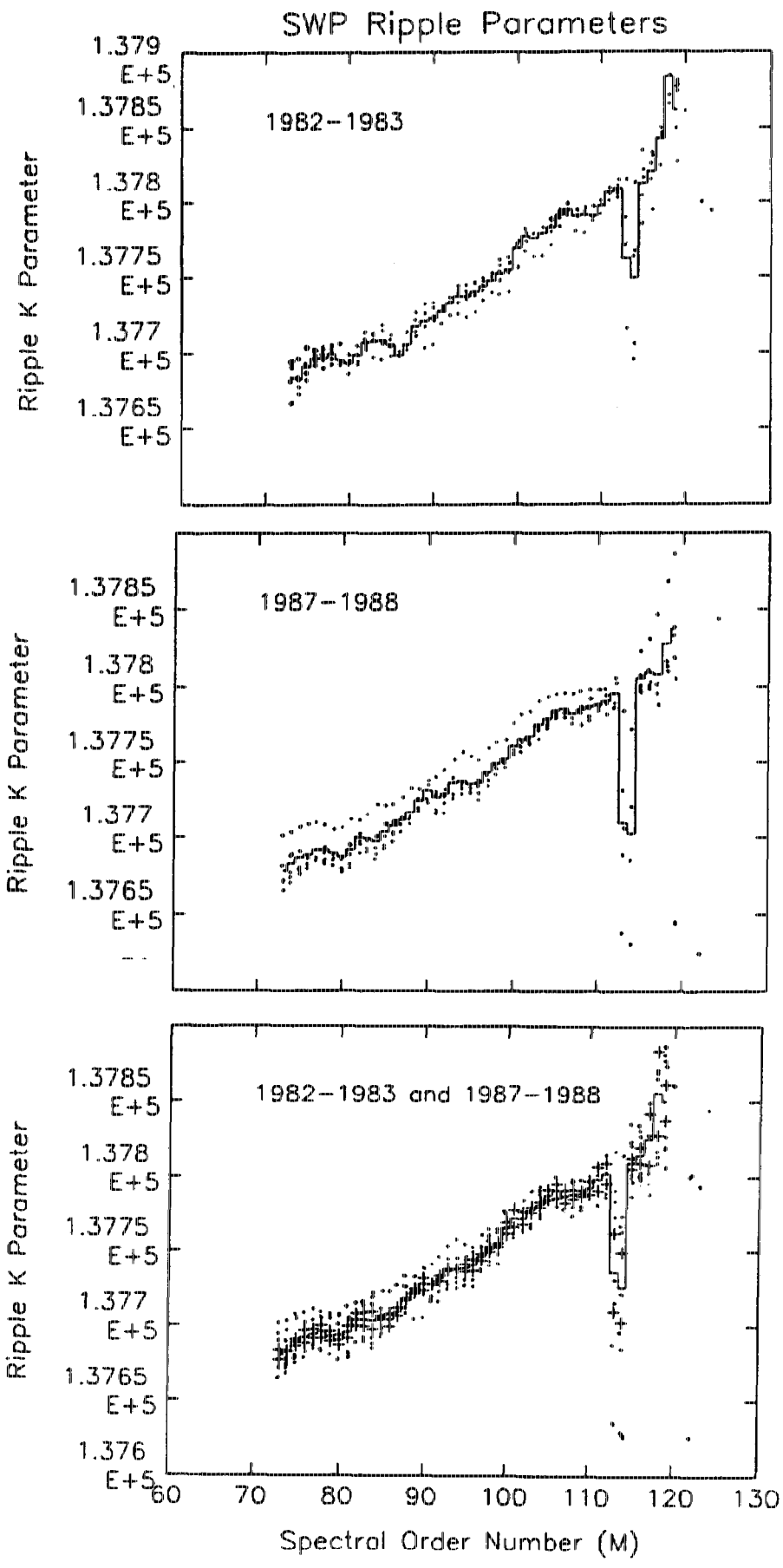
SWP Ripple Parameters
1982-1983
1987-1988
1982-1983 and 1987-1988
Ripple K Parameter
1.379 E+5
1.3785 E+5
1.378 E+5
1.3775 E+5
1.377 E+5
1.3765 E+5
1.376 E+5
60
70
80
90
100
110
120
130
Spectral Order Number (M)

Figure 2

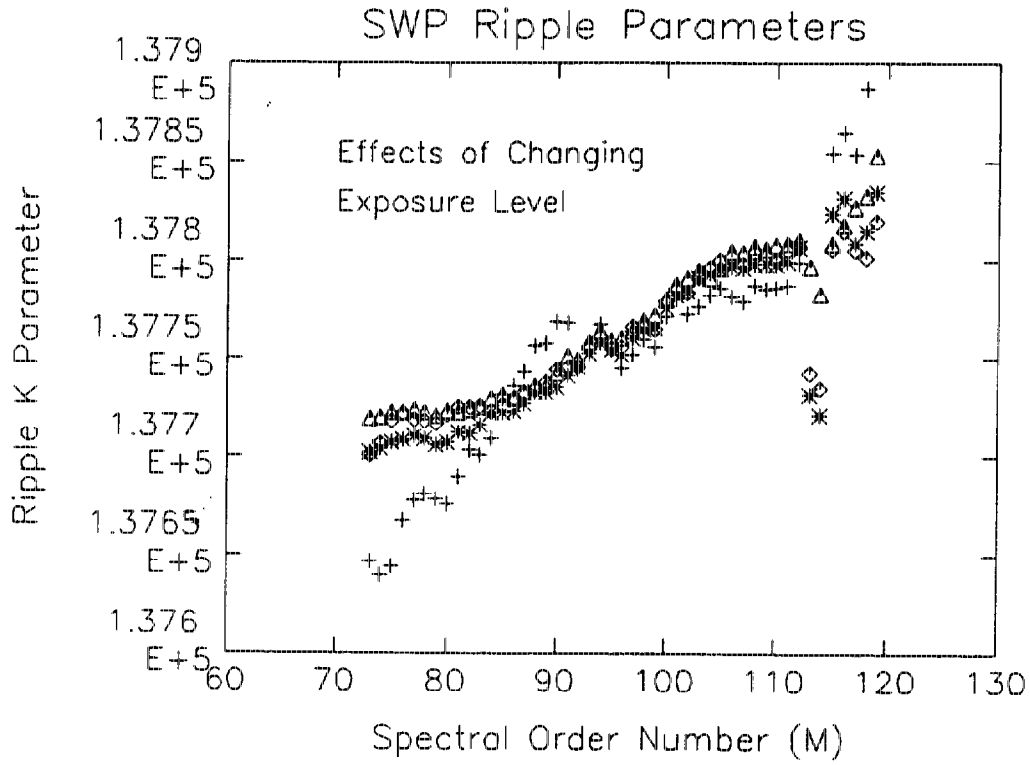

Figure 3

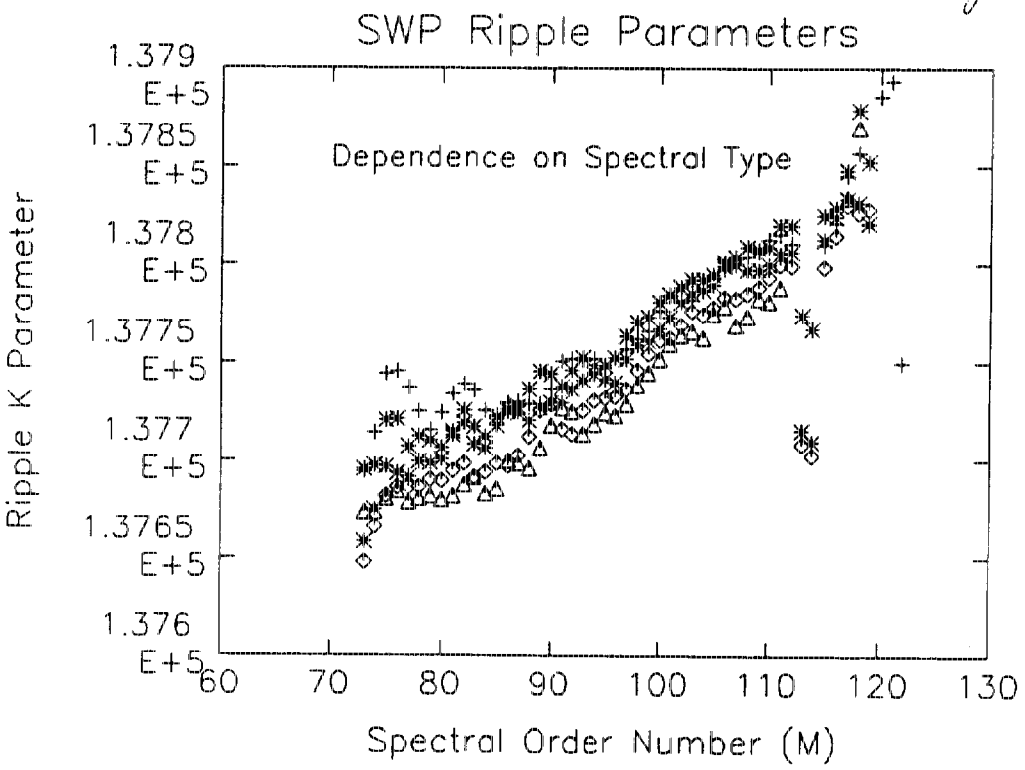

Figure 4

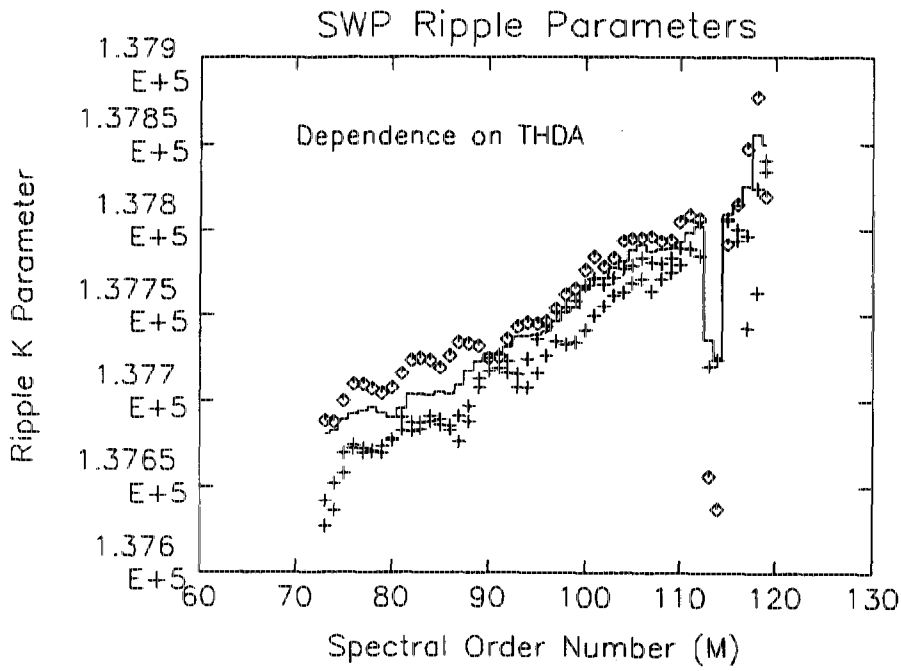
SWP Ripple Parameters
Dependence on THDA
Ripple K Parameter
1.379 E+5
1.3785 E+5
1.378 E+5
1.3775 E+5
1.377 E+5
1.3765 E+5
1.376 E+5
60
70
80
90
100
110
120
130
Spectral Order Number (M)

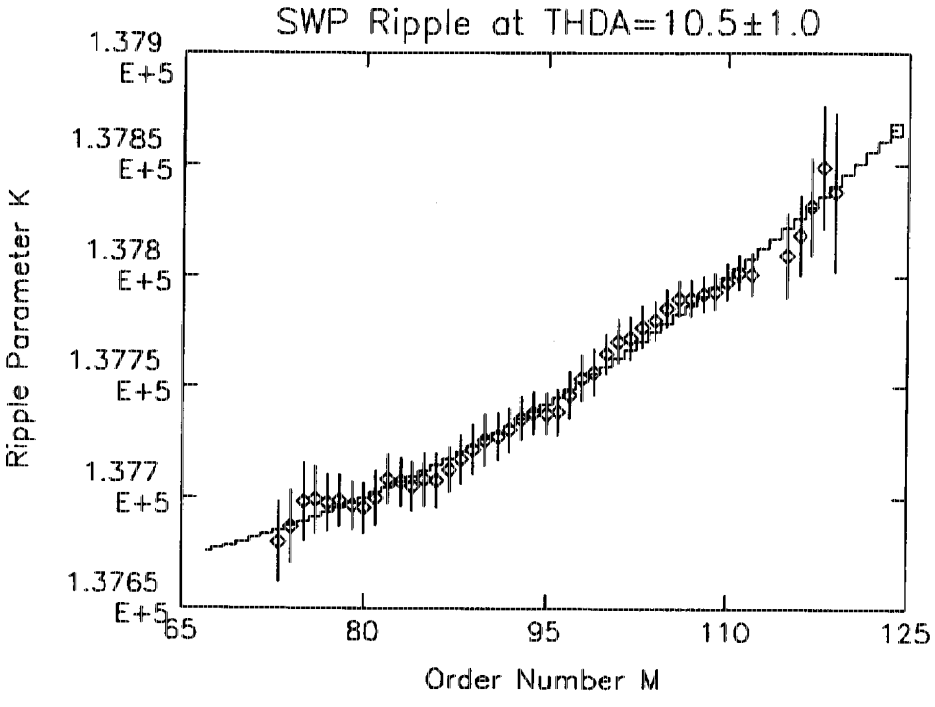

Figure 5a

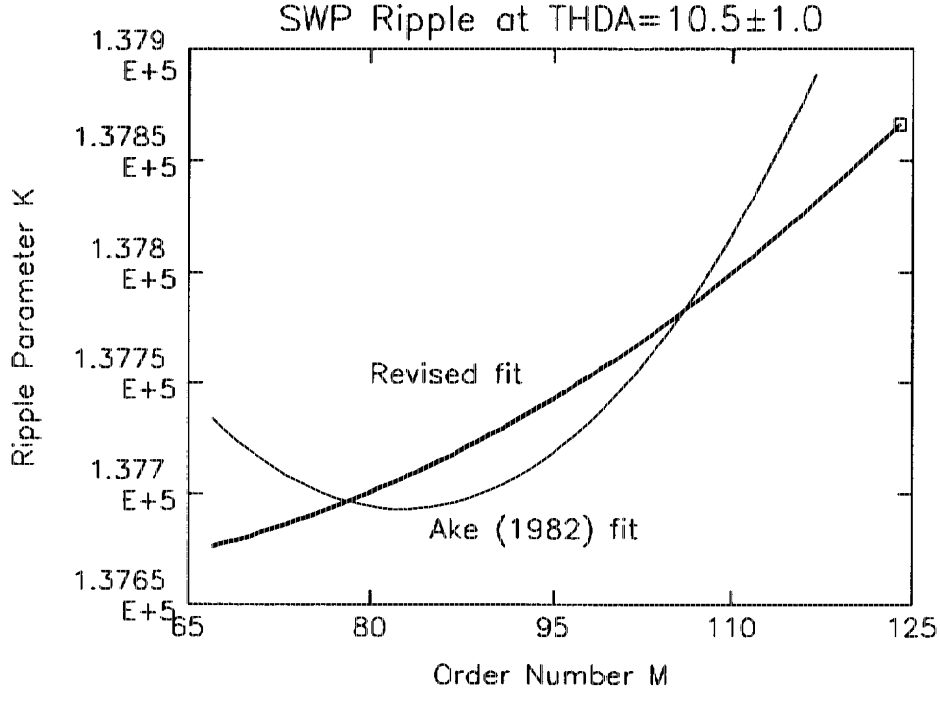

Figure 5b

Figure 6a

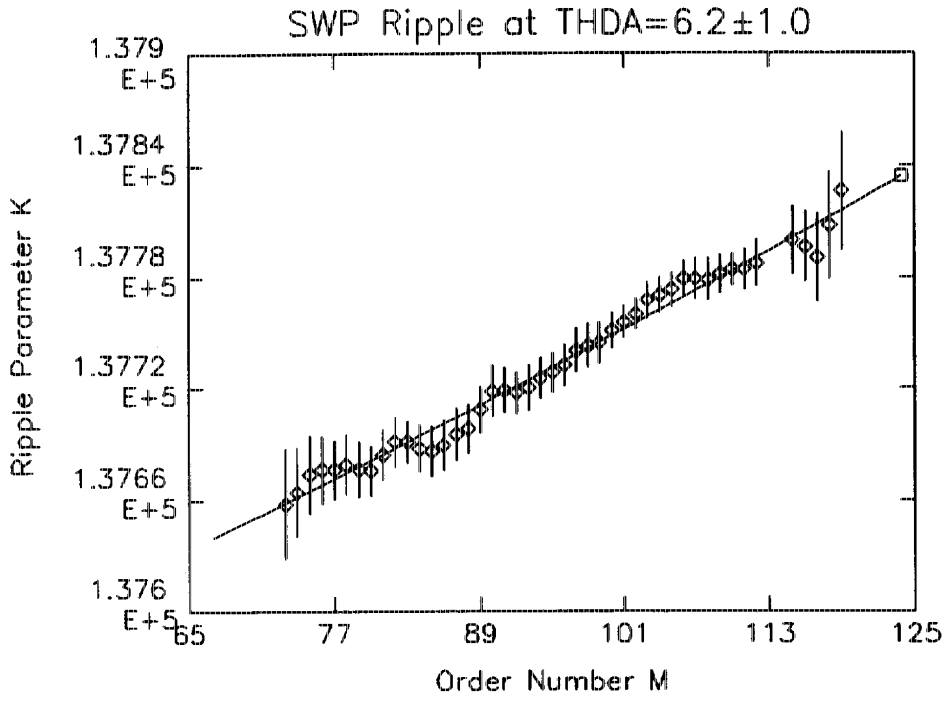

Figure 6b

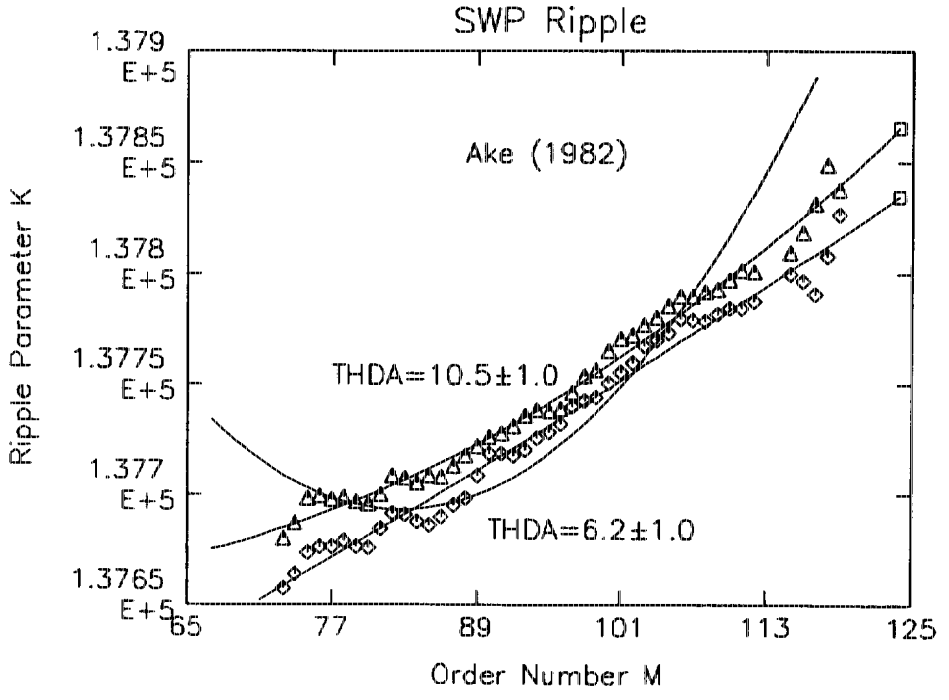

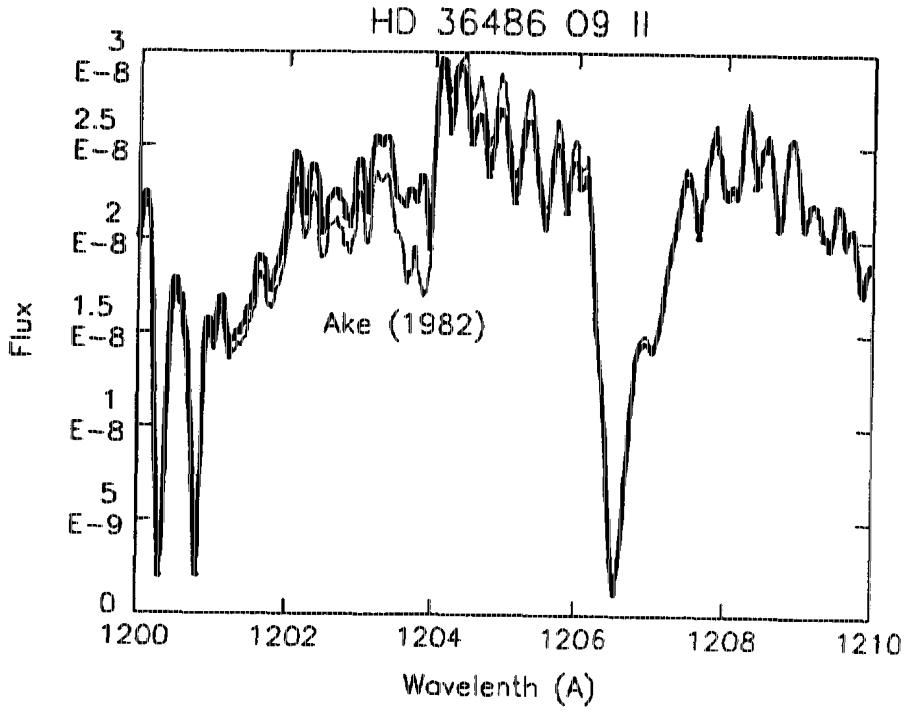
HD 36486 O9 II
Ake (1982)
Flux
3 E-8
2.5 E-8
2 E-8
1.5 E-8
1 E-8
5 E-9
0
1200
1202
1204
1206
1208
1210
Wavelenth (A)

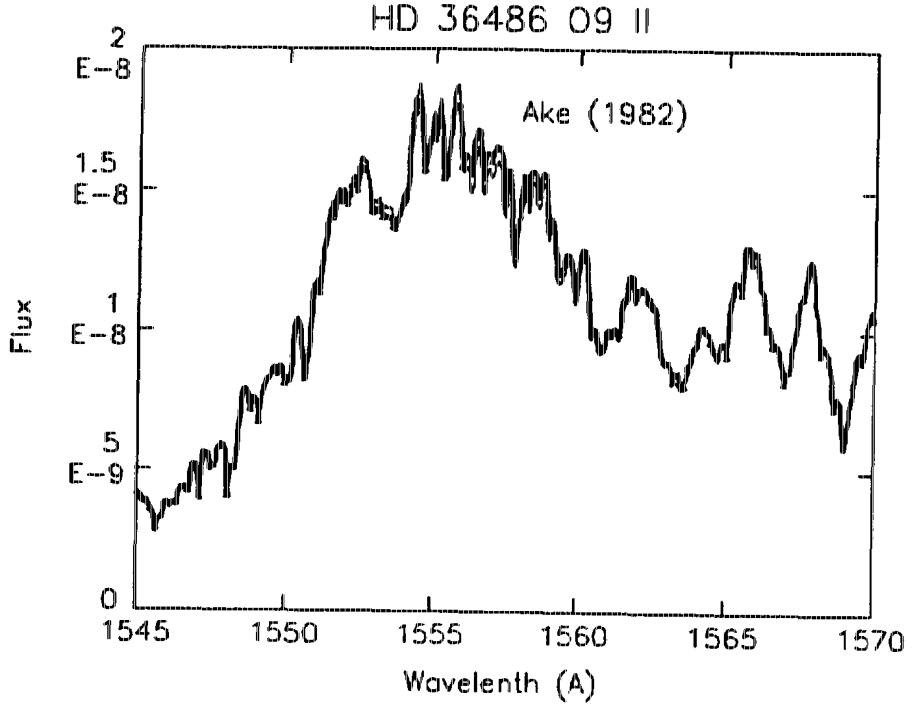
HD 36486 O9 II
Ake (1982)
Flux
2 E-8
1.5 E-8
1 E-8
5 E-9
0
1545
1550
1555
1560
1565
1570
Wavelenth (A)

Fig 7b

Fig 7c

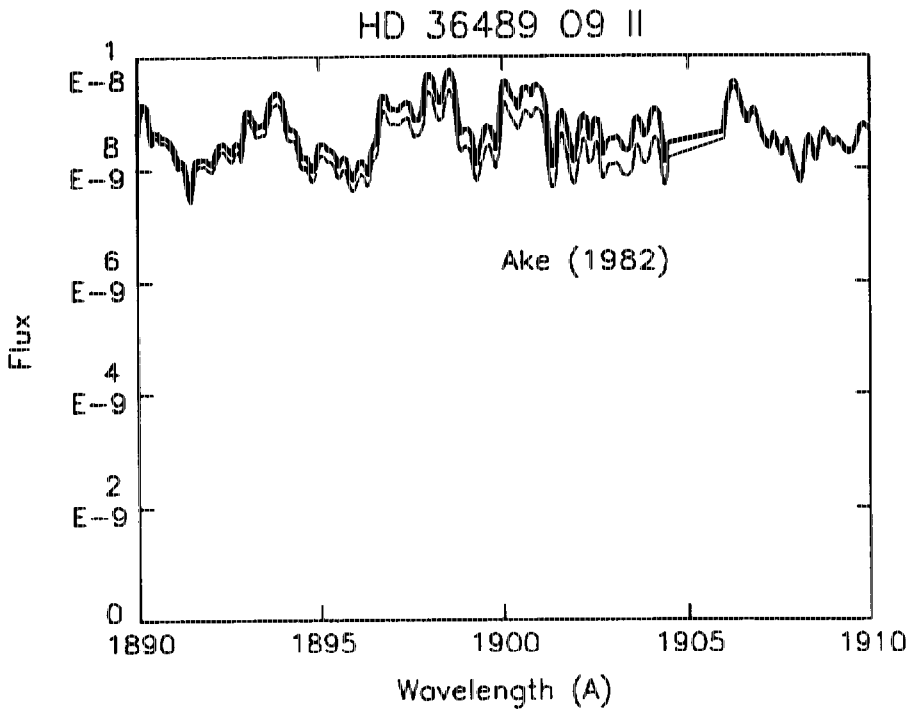
HD 36489 O9 II
Ake (1982)
Flux
1 E-8
8 E-9
6 E-9
4 E-9
2 E-9
0
1890
1895
1900
1905
1910
Wavelength (A)

Fig 7d

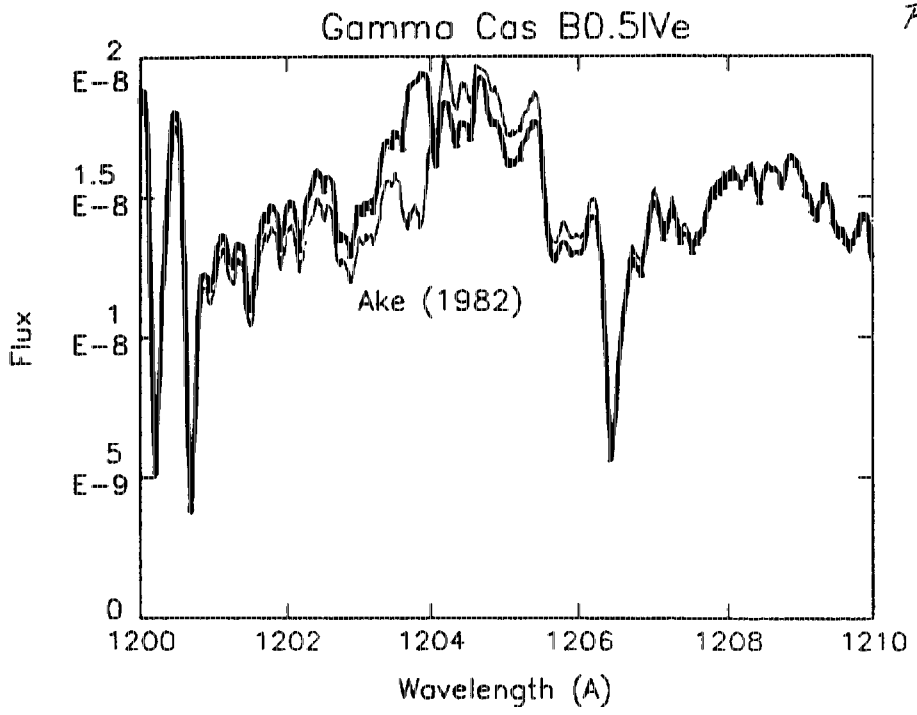
Gamma Cas B0.5IVe
Ake (1982)
Flux
2 E-8
1.5 E-8
1 E-8
5 E-9
0
1200
1202
1204
1206
1208
1210
Wavelength (A)

fig 7e

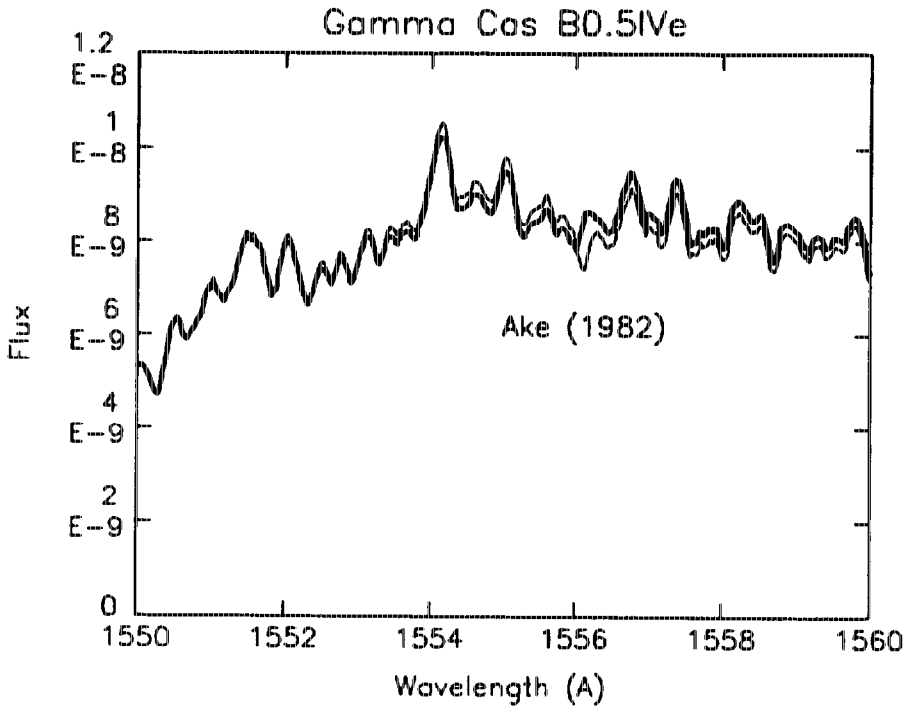
Gamma Cas B0.5IVe
1.2 E-8
1 E-8
8 E-9
6 E-9
4 E-9
2 E-9
0
Flux
Ake (1982)
1550
1552
1554
1556
1558
1560
Wavelength (A)

fig 7f

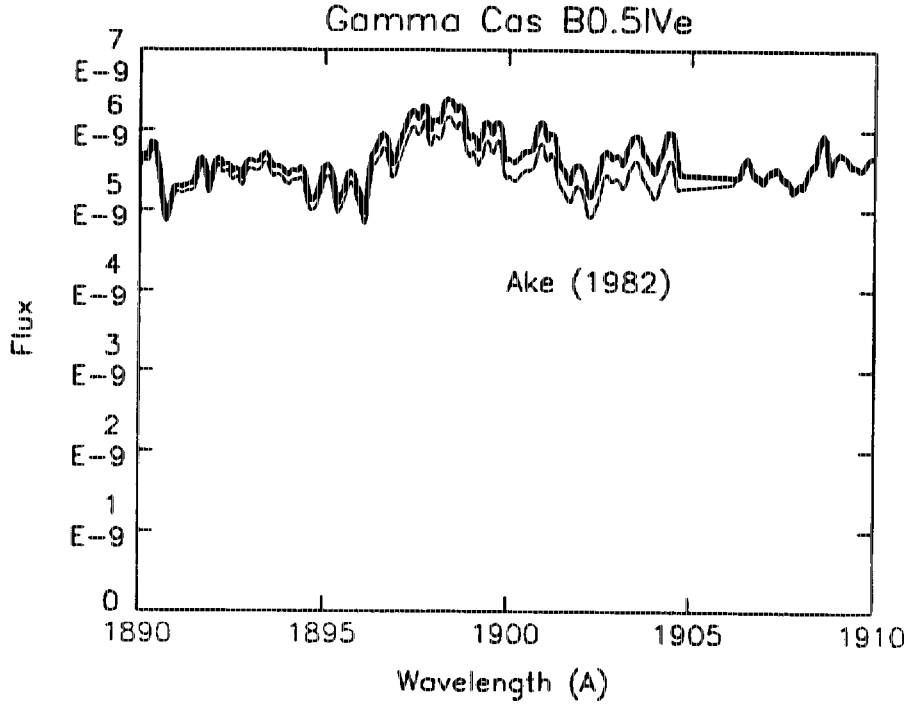
Gamma Cas B0.5IVe
7 E-9
6 E-9
5 E-9
4 E-9
3 E-9
2 E-9
1 E-9
0
Flux
Ake (1982)
1890
1895
1900
1905
1910
Wavelength (A)

Fig 7g

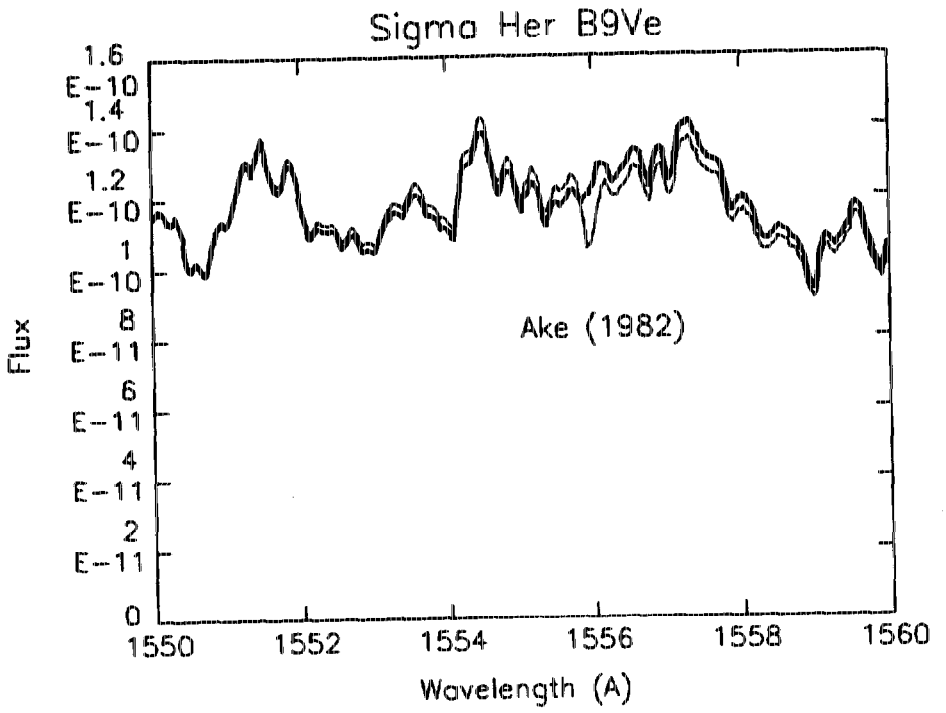
Sigma Her B9Ve
Flux
1.6 E-10
1.4 E-10
1.2 E-10
1 E-10
8 E-11
6 E-11
4 E-11
2 E-11
0
Ake (1982)
1550
1552
1554
1556
1558
1560
Wavelength (A)

Fig 7h

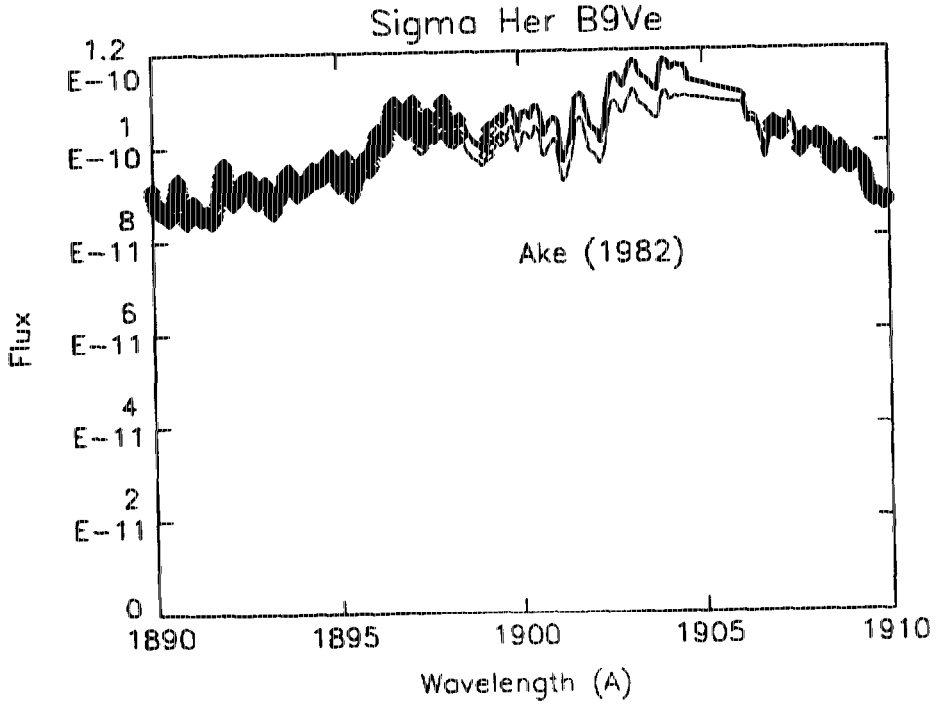
Sigma Her B9Ve
Flux
1.2 E-10
1 E-10
8 E-11
6 E-11
4 E-11
2 E-11
0
Ake (1982)
1890
1895
1900
1905
1910
Wavelength (A)